Article

Combustion Characterization and Kinetic Analysis of Mixed Sludge and Lignite Combustion

Yang Sun,* Hui Sun, Tianhua Yang, Yiming Zhu, and Rundong Li

Read Online

ACCESS | Metrics & More | Article Recommendations

ABSTRACT: To investigate the feasibility and reaction mechanism of combusting sewage sludge and brown coal in a mixture. Thermal behavior evaluation of combustion characteristics, interactions, and kinetic analysis of sludge-lignite mixture combustion by thermogravimetry (TG). The results showed that the combustion performance of the mixed samples was all in between that of the lignite and sludge samples. The combined combustion index gradually decreased with the increase in sludge mixing. The addition of sludge favors the ignition of the mixture but is not conducive to overall stable combustion. The synergies between the sludges, as assessed by the mass loss curves, are reflected in the ash removal and coke oxidation stages. When the mixture of sludge and lignite is burned at a ratio of 10 wt %, the calorific value can still reach 20.3 MJ/kg, which is only about 4.2% lower than that of burning lignite alone. Application of the kinetic models of FWO, Starink, KAS, and Friedman, in turn, determined a minimum average activation energy of only 132.50 kJ/mol. In addition, the reaction was judged to be a simple complexation reaction by analyzing the thermodynamic parameters (ΔG, ΔS, ΔH, and A), with the combustion process approaching thermodynamic equilibrium and forming stable products. The nucleation model A4.2 can be used as the best reaction mechanism model for sludge−lignite mixed combustion.
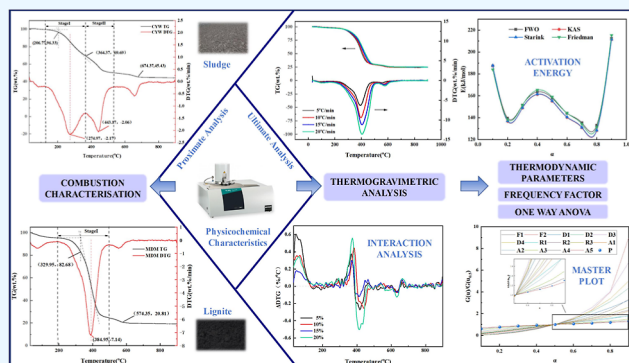
1. INTRODUCTION

Coal is one of the most commonly used fossil fuels, and the energy released from its combustion can be used for various applications, including generating electricity and heating. China's coal resources are mainly located in Shanxi, Shaanxi, and Inner Mongolia. Among them, Inner Mongolia lignite, which is huge in quantity, is characterized by high moisture content, low calorific value, and low sulfur content.

Sludge is a byproduct of municipal and industrial wastewater treatment and is routinely discharged, causing air pollution and unpleasant odors. The presence of heavy metals, pathogens, and difficult-to-decompose organic compounds leads to secondary contamination of soil and water sources by conventional sludge landfills. Second, the high ash content, low calorific value, and poor combustion stability of sludge after drying make it difficult to burn and utilize it alone. To reduce the use of coal and enhance sludge treatment, suitable equipment and processes for mixing and combusting both fuels are necessary. Therefore, investigating the miscibility characteristics of two low-order fuels provides a basis for realizing efficient and low-pollution combustion regulation strategies.[1]

Based on the literature reports with actual coal-fired power plant combustion, the percentage of dried sludge is generally below 10%. For example, Zhao et al.[2] explored that a sludge and bituminous coal blending ratio of 10% moisture content to 50% is feasible for ash caking tendency, SO_2, and heavy metal emissions. However, HCN and N_2O emissions will gradually increase. Hao et al.[3] mixed combustion of tannery sludge and coal in a commercial circulating fluidized bed boiler at a 30% ratio of sludge. Emissions of gaseous pollutants and the distribution of heavy metals in various types of ash were studied. Qi et al.[4] blended sludge with high sodium coal at large blending ratios and analyzed the ignition and combustion performance with increasing moisture content. Wang et al.[5] focused on combustion behavior and kinetics. Wang et al.[6] focused on the synergistic behavior and mineral transformation of coal and sludge. Jeong Min Park et al.[7] reported that dried sludge can be confirmed at up to 20% without a significant impact on gas emissions. However, none of the above articles analyze and evaluate the thermal behavior of specific fuel blends. In this paper, the optimal mixing ratio and the optimal reaction mechanism model are investigated by combining

sludge and lignite combustion characteristics with kinetics and thermodynamics. To provide a reference for the combustion of sludge mixed with lignite, which are low-ranking fuels.

In summary, the characterization and kinetic analysis of the combustion of sludge and lignite mixtures is one of the most popular research areas currently. The in-depth study of the characteristics and reaction mechanisms of mixed fuels[8] can make a positive contribution to the optimization of combustion technology, the improvement of energy efficiency, and the protection of the environment.

Kinetic and thermodynamic studies of sludge and lignite pyrolysis. Enrichment of their utilization potential for energy and byproduct recovery. Given the knowledge gap on coal resources, this study combines TG and modeling techniques to dynamically characterize the mixing and combustion drivers, behaviors, kinetics, thermodynamics, and reaction mechanisms of two low-rank fuels. The combustion performance of sludge, lignite, and their mixed samples in different proportions was evaluated by burning them at different heating rates in a TG tester. The synergistic and inhibitory effects of the reactions were judged by calculating interactions. Evaluate the stability of combustion with respect to heat generation and transfer using thermodynamic parameters. Additionally, kinetic calculations using nonisothermal isoconversion techniques were carried out to establish the reaction's minimal activation energy. Moreover, choosing the best reaction mechanism model for the lignite and sludge combustion. To provide a basis for realizing an efficient and low-pollution combustion regulation strategy for sludge and lignite.

2. MATERIALS AND METHODS

2.1. Sample Preparation and Characterization. The sludge (CYW) samples used in this study with 80% water content were obtained from the Chaoyang area, China. Lignite (MDM) samples were obtained from the eastern part of Inner Mongolia, China. First, the sludge and lignite were heated at 105 °C for 24 h in a blower drying oven. The dried sludge and lignite samples were then broken up and sieved by using a pulverizer to create a sample with a particle size of less than 100 mesh. Finally, sealed plastic bags containing dried samples designed with sludge mass percentages of 5, 10, 15, and 20 wt % were stored. Table 1 contains the findings of industrial analysis (GB/T28731-2012) and elemental analysis (GB/T31391-2015).

Table 1. Industrial and Elemental Analyses of Sludge and Lignite Samples

sample		CYW	MDM
industrial analysis (wt %)	M	2.14	2.86
	V	48.26	34.49
	FC	3.94	41.21
	A	45.67	21.45
	V/FC	12.26	0.84
elemental analysis (wt %)	C	25.56	50.99
	H	3.76	3.90
	N	4.05	0.93
	O	18.06	18.98
	S	0.77	0.90
	C/H	6.79	13.10
calorific value (MJ/kg)		10.99	21.20

The sludge samples had a rather high volatile matter and ash concentration, as can be observed in Table 1. On the other hand, the fixed and elemental C contents of the lignite samples were both relatively high. Each sample's calorific value was determined using an oxygen bomb calorimeter, and it is clear that the lignite sample has a far higher calorific value than the sludge sample. A modest amount of sludge added to the mixture, however, has no discernible impact on the fuel's overall calorific value. With a mixing ratio of 10%, the calorific value can still reach 20.3 MJ/kg, which is only about 4.2% lower than the calorific value of burning lignite alone. In addition, the sludge sample had a C/H mass ratio of 6.79 and a V/FC mass ratio of 12.26. The high volatile matter of sludge promotes fuel ignition compared to 13.10 and 0.84 of lignite.

2.2. TG Analysis. The samples were weighed (8 ± 0.001 mg) into an Al_2O_3 crucible and tested by simultaneous TG methods. The instrument (Netzsch STA449F3) was tested to an accuracy of 10^{-7} g. The experiments were conducted in an environment of air, with a volume flow rate of 100 mL/min. Samples were heated at rates of 10, 15, 20, and 25 °C/min from room temperature to 900 °C. The first-order derivative and thermogravimetric data curves (TG and DTG) were analyzed for each sample during combustion in this temperature range.

2.3. Combustion Characteristic Parameters. Evaluation of the combustion performance of the fuel needs to be judged by the ignition index (C_s, wt %/min^3), the burnout index (C_f, wt %/min^4), and the combined combustion index (S, wt %^{2}/(°C^3 min^2)). Equations 1−3 were used to calculate these parameters. The ignition temperature (T_s, °C), burnout temperature (T_f, °C), and peak temperature (T_m, °C) were three significant parameters used to assess the combustion properties of the fuel and were acquired by TG and DTG curves[9]

$$C_s = \frac{(d_w/d_t)_{max}}{t_s t_{max}} \tag{1}$$

$$C_f = \frac{(d_w/d_t)_{max}}{\Delta t_{1/2} t_{max} t_f} \tag{2}$$

$$S = \frac{(d_w/d_t)_{max}(d_w/d_t)_{mean}}{T_s^2 T_f} \tag{3}$$

where t_s represents the time corresponding to the ignition temperature, t_f represents the time corresponding to the burnout temperature, and t_m represents the time corresponding to the peak temperature. (d_w/d_t) mean represents the average mass loss rate (wt %/min) and (d_w/d_t) max represents the maximum mass loss rate (wt %/min). $\Delta t_{1/2}$ represents the time (min) between two points on the corresponding DTG curve when $(d_w/d_t)/(d_w/d_t)$ max is 1/2.

2.4. Mixed Combustion Interactions. The interaction between the components was elucidated by experimental and calculated TG curves.[10] The weight loss rate and cumulative gas production of mixed combustion are not a simple superposition of pure sludge and lignite values. Rather, the presence of synergistic and inhibitory effects can be seen by comparing the difference between the measured and calculated values

$$W_{cal} = k_1 W_1 + k_2 W_2 \tag{4}$$

Table 2. Four Methods of Kinetic Analysis

model	equation	graph
Flynn−Wall−Ozawa (FWO)	$\ln(\beta) = \ln\left(\dfrac{AE}{RG(\alpha)}\right) - 5.331 - 1.052\left(\dfrac{E}{RT}\right)$	$\ln(\beta) \text{ vs } \dfrac{1}{T}$
Kissinger−Akahira−Sunose (KAS)	$\ln\left(\dfrac{\beta}{T^2}\right) = \ln\left(\dfrac{AE}{RG(\alpha)}\right) - \dfrac{E}{RT}$	$\ln\left(\dfrac{\beta}{T^2}\right) \text{ vs } \dfrac{1}{T}$
Starink	$\ln\left(\dfrac{\beta}{T^{1.92}}\right) = \ln\left(\dfrac{AE}{RG(\alpha)}\right) - 0.0312 - 1.0008\dfrac{E}{RT}$	$\ln\left(\dfrac{\beta}{T^{1.92}}\right) \text{ vs } \dfrac{1}{T}$
Friedman	$\ln\left(\beta\dfrac{d\alpha}{dt}\right) = \ln(f(\alpha)A_\alpha) - \left(\dfrac{E_\alpha}{RT}\right)$	$\ln\left(\dfrac{d\alpha}{dt}\right) \text{ vs } \dfrac{1}{T}$

Equation 4, where W_1 and W_2 represent measured values of the mass loss ratios of sludge and lignite when burned separately under the same conditions as mixed combustion. W_{cal} is the calculated value for mixed combustion under the same conditions. k_1 and k_2 represent the mass fractions of sludge and lignite

$$\Delta DTG = DTG_{exp} - DTG_{cal} \tag{5}$$

Equation 5, where ΔDTG represents the deviation of the experimental value from the calculated value of the rate of mass loss of the blend. DTG_{exp} represents the experimental value of the TG rate and DTG_{cal} represents the calculated value of the TG rate. $\Delta DTG > 0$ and $\Delta DTG < 0$ represent inhibitory and synergistic effects.[11]

2.5. Kinetic Analysis. Investigating reaction mechanisms, processes, and temperature determination heavily rely on the kinetic parameters. Kinetic analyses are widely used to understand the combustion process and thermodynamic characteristics of sludge and lignite. Over time, numerous computational techniques have been created and improved. Thermodynamic parameters can be determined using the Flynn−Wall−Ozawa (FWO), Kissinger−Akahira−Sunose (KAS), Starink, and Friedman methods.[12] Among these, the equivalent conversion rate technique has a good reference value for the production process and calculates outcomes with high precision. Although different approaches result in different calculations, these variations are frequently acceptable in the final outcome. The four approaches are used not only to check the computations' accuracy but also to compare them. Thus, the most similar sludge and lignite combustion models are found. To make the results of the study favorable for evaluating the reactivity and kinetic mechanisms of mixed combustion.

The kinetics of sludge, lignite, and mixed samples were investigated using a nonisothermal isoconversion method. Using these methods, activation energy E and prefactor A were identified. Temperature and conversion rate affect the rate of mass loss, which can be expressed as follows in eq 6

$$\frac{d\alpha}{dt} = k(T)f(\alpha) \tag{6}$$

where T stands for the absolute temperature, $k(T)$ is the reaction rate constant, $f(\alpha)$ is the reaction mechanism function, and α is the conversion rate. $k(T)$ and α are expressed according to the Arrhenius eqs 7 and 8

$$k(T) = A\exp\left(-\frac{E}{RT}\right) \tag{7}$$

$$\alpha = \frac{m_0 - m_t}{m_0 - m_\infty} \tag{8}$$

where R is the gas constant, A is the prefinger factor, and E is the activation energy. The initial mass is denoted by m_0, the temperature-dependent mass is denoted by m_t, and the final mass is denoted by m_∞.

The rate of warming β heating rate can be defined as the rate of change of temperature with respect to time and can be expressed as eq 9

$$\beta = \frac{dT}{dt} \tag{9}$$

Combining the above equations finally yields eq 10

$$\frac{d\alpha}{f(\alpha)} = \frac{A}{\beta}\exp\left(-\frac{E}{RT}\right)dT \tag{10}$$

Equation 10 is obtained by integrating the initial condition $\alpha = 0$ with $T = T_0$ eq 11

$$G(\alpha) = \int_0^\alpha \frac{d\alpha}{f(\alpha)} = \frac{A}{\beta}\int_0^T \exp\left(-\frac{E}{RT}\right)dT \tag{11}$$

Table 2[13] represents various isoconversional models with their respective equations and slopes to find out activation energy and frequency factor, which have been employed in this investigation. KAS, FWO, and Starink are integral methods whereas Friedman is a differential method. The activation energy can be evaluated from the slope of the graph. The isoconversional models are used to calculate activation energy. The apparent activation energy of thermodynamic parameters A, ΔH, ΔG, and ΔS were estimated by eqs 12−15

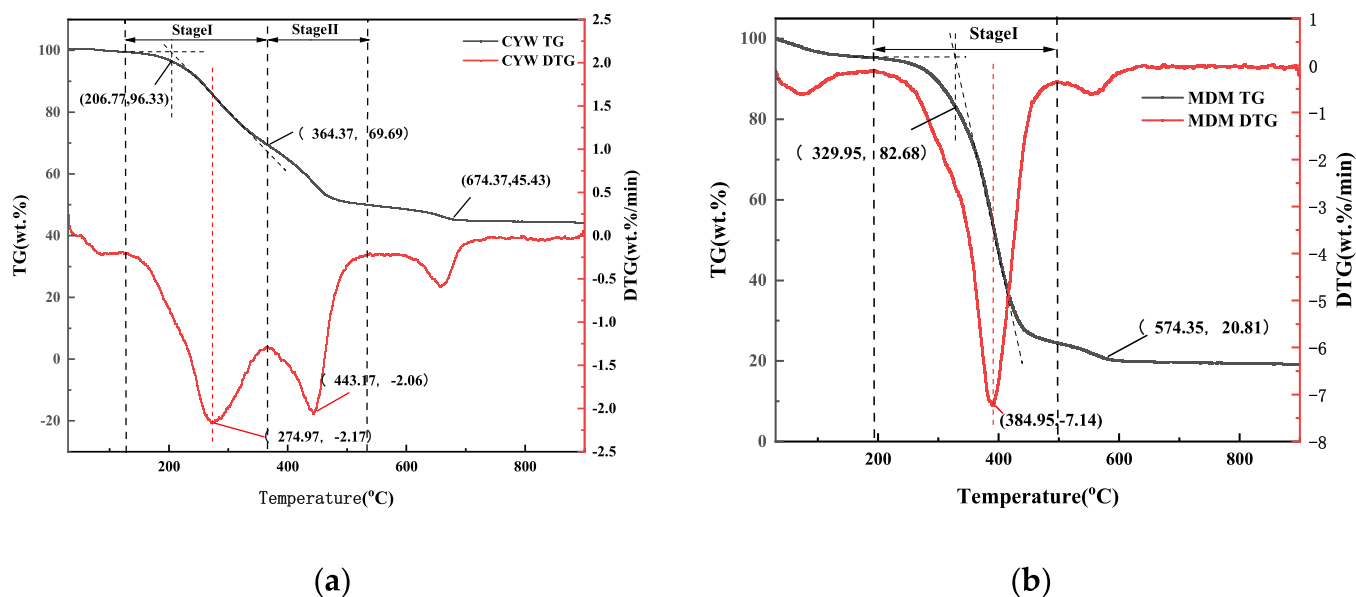$$A = \frac{\left[\beta E_\alpha \exp\left(\frac{E_\alpha}{RT_m}\right)\right]}{RT_m^2} \tag{12}$$

$$\Delta H = E_\alpha - RT \tag{13}$$

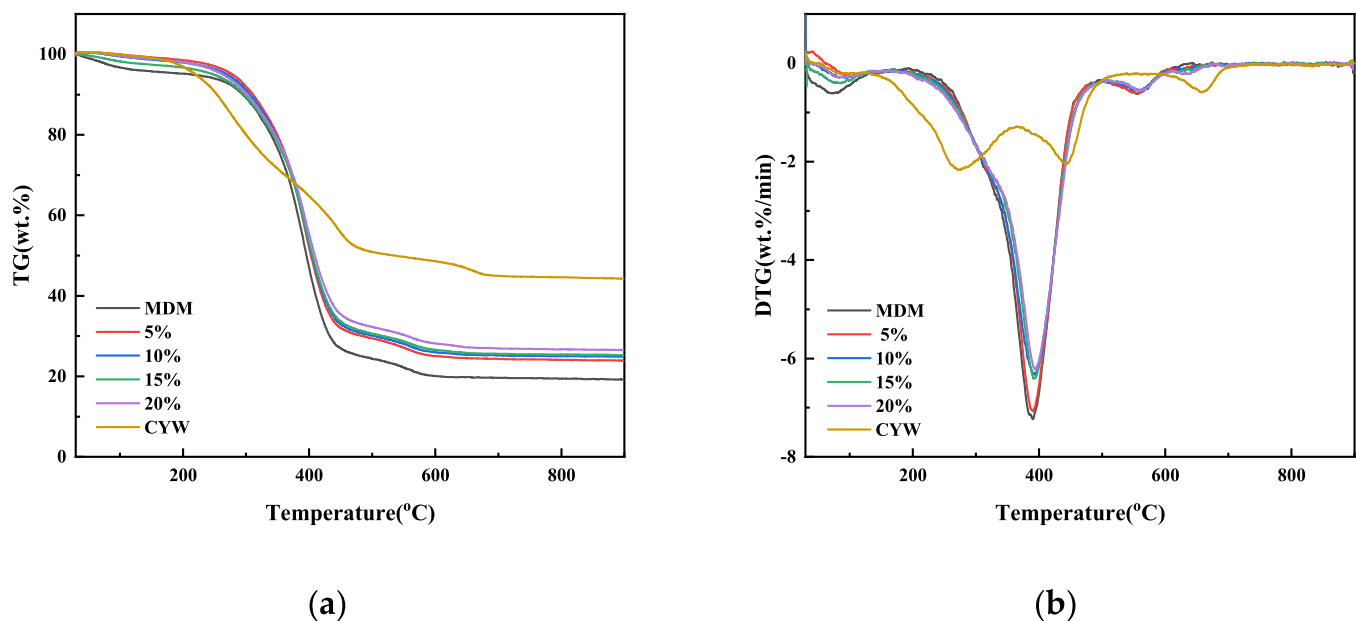$$\Delta G = E_\alpha + RT_m \cdot \ln\left(\frac{K_B T_m}{hA}\right) \tag{14}$$

$$\Delta S = \frac{\Delta H - \Delta G}{T_m} \tag{15}$$

where K_B and h are Boltzmann's constant $(1.381 \times 10^{-23}$ J/K) and Planck's constant $(6.626 \times 10^{-34}$ J·s).

Using E_α estimation based on FWO, KAS, Starink, Friedman, and the master plot method, the most appropriate

Figure 1. TG-DTG curves of sludge and lignite samples combusted at 10 °C/min in an air atmosphere. (a) Sludge and (b) lignite.

Figure 2. TG and DTG curves of sludge, lignite, and mixed samples at a temperature increase rate of 25 °C/min. (a) TG and (b) DTG.

response mechanism can be identified. Equation 11 can be transformed into

$$G(\alpha) = \frac{AE}{\beta R} P(u) \tag{16}$$

$P(u)$ is the temperature integral function, $u = E/RT$, and by Doyle's approximation, $P(u)$ can be transformed into the following form

$$P(u) = 0.00484\exp(-0.1051u) \tag{17}$$

Choosing $\alpha = 0.5$ as the interval point, eq 16 becomes

$$G(0.5) = \frac{AE}{\beta R} p(u_{0.5}) \tag{18}$$

$G(0.5)$ represents the value corresponding to the mechanism function in integral form when $\alpha = 0.5$ and $u_{0.5} = E/RT_{0.5}$; $T_{0.5}$ represents the temperature at $\alpha = 0.5$.

Combining eqs 17 and 18, the master plot integral equation can be transformed as

$$\frac{G(\alpha)}{G(\alpha_{0.5})} = \frac{p(u)}{p(u_{0.5})} \tag{19}$$

eq 19, the left side of the equation, $G(\alpha)/G(\alpha_{0.5})$, can be determined from the mechanism functions in the table, while the right side of the equation, $P(u)/P(u_{0.5})$, can be calculated from experimental data. By comparing the theoretical and practical master plots, it is possible to determine the reaction mechanism and function of the combustion process.

3. RESULTS

3.1. Analysis of Sludge and Lignite Combustion Alone. Figure 1 presents the TG curves of the separate

Table 3. Common Reaction Mechanisms and Integral Forms[14]

symbol	reaction mechanisms	$f(\alpha)$	$G(\alpha)$
	Nucleation growth model		
A1	one-dimensional	$1.5(1-\alpha)[-\ln(1-\alpha)]^{1/3}$	$[-\ln(1-\alpha)]^{2/3}$
A2	two-dimensional	$2(1-\alpha)[-\ln(1-\alpha)]^{1/2}$	$[-\ln(1-\alpha)]^{1/2}$
A3	three-dimensional	$3(1-\alpha)[-\ln(1-\alpha)]^{2/3}$	$[-\ln(1-\alpha)]^{1/3}$
	Diffusion		
D1	one-dimension transport	$1/(2\alpha)$	α^2
D2	two-dimension transport	$[-\ln(1-\alpha)]^{-1}$	$(1-\alpha)\ln(1-\alpha)+\alpha$
D3	three-dimension transport	$(3/2)(1-\alpha)^{2/3}[1-(1-\alpha)1/3]^{-1}$	$[1-(1-\alpha)^{1/3}]^2$
D4	Ginstling–Brounstein equation	$(3/2)[(1-\alpha)^{-1/3}-1]^{-1}$	$(1-2\alpha/3)-(1-\alpha)^{2/3}$
	Order of reaction		
F1	first-order	$1-\alpha$	$-\ln(1-\alpha)$
F2	second-order	$(1-\alpha)^2$	$(1-\alpha)^{-1}-1$
F3	third-order	$(1-\alpha)^3$	$[(1-\alpha)^{-2}-1]/2$
F4	fourth-order	$(1-\alpha)^4$	$[(1-\alpha)^{-3}-1]/3$
	Geometrical contraction model		
R1	one-dimensional	1	α
R2	two-dimensional	$2(1-\alpha)^{1/2}$	$1-(1-\alpha)^{1/2}$
R3	three-dimensional	$3(1-\alpha)^{2/3}$	$1-(1-\alpha)^{1/3}$

sludge and lignite samples combusted in an air atmosphere at a heating rate of 10 °C/min. Without considering the precipitation of free and bound water near 100 °C,[15] sludge weight loss can be divided into two stages. The first stage, from 206.77 to 364.37 °C, corresponds mainly to the decomposition of organic compounds with weak chemical bonds, such as carbohydrates and aliphatic compounds.[16] The second stage, from 364.37 to 674.37 °C, is dominated by the decomposition of organic substances with strong chemical bonds, such as some aromatic compounds and the oxidative combustion of charcoal. There is also a small weight loss of about 2% that occurs after the temperature reaches 674.34 °C, which is a loss of mass due to the decomposition of the residue. The combustion processes of coal and sludge are significantly different. Lignite coal loses weight in only one stage, from 329.95 to 574.35 °C. It occurred mainly with the combustion of volatile matter and carbon and the depolymerization of the

dense polycyclic aromatic hydrocarbons that make up coal. The last 500 ~574.35 °C is the side-shoulder precipitation peak of volatile components. The mass of sludge is essentially unchanged after 700 °C, and the mass of coal is essentially unchanged after 600 °C. The weight loss on combustion of sludge and lignite finally went to 44.31 and 19.20 wt %.

The sludge has an ignition temperature of 206.77 °C and burnout temperatures of 206.77 and 674.37 °C. In contrast, lignite has an ignition temperature of 329.95 °C and a burnout temperature of 574.35 °C. In contrast, the ignition temperature of sludge is relatively low, mainly because the chemical bonds of small molecular compounds in sludge are easier to break. Higher temperatures are often required for polymerization bond breaking in lignite. The relatively high combustion temperature also contributes to excessive heavy metal residues in the sludge. The average and maximum rates of weight loss during the weight loss phase are smaller than those of lignite. This is also combined with the fact that the fixed carbon content of sludge is much lower than that of lignite, while the combustion performance of sludge is worse than that of lignite.[17]

3.2. Analysis of Mixed Combustion of Sludge and Lignite. The TG and DTG curves for 25 °C/min combustion of sludge, lignite, and mixed fuels are shown in Figure 2. It can be seen that the combustion characteristics of blended fuels are intermediate between those of individual fuels. Also, as the sludge blending ratio increased, the mass loss advanced, but the loss became less. In addition to this, the mixture also tends to show a two-stage mass loss as the sludge mass fraction increases with the sludge combustion curve.[18] The incorporation of a 5 wt % proportional blend of fuel was similar to the rate of combustion of lignite alone, but the mass loss was still significantly different. The combustion rate and mass loss do not vary much in the range of 10−20 wt %, and combustion is acceptable up to 20 wt % proportional mixing.

Table 4 displays the sludge, lignite, and mixed fuel combustion characteristics. As the sludge blending ratio increases, the rate of mass loss of the mixed fuel gradually reduces. Sludge ignites at a temperature that is 123.18 °C lower than lignite. This suggests that lignite is less reactive than sludge.[19] Bond-breaking reactions start to happen as soon as the lignite is lit, and some free radical fragments are also created. The breakdown of cross-linked aromatic hydrocarbons in lignite is aided by the reaction between these reactive radicals.[20]

From Table 5, it can be seen that with the gradual increase in the proportion of sludge blending, the ignition temperature is decreasing and the combustion temperature is increasing. However, by mixing 20 wt % of sludge, the ignition temperature also changed by only 2.51 °C, which has a small effect. The ignition index also indicates that the addition of

Table 4. Characteristic Parameters of Combustion for Sludge, Lignite, and Mixed Samples

combustion characteristics	MDM	5 wt %	10 wt %	15 wt %	20 wt %	CYW
T_m (°C)	384.95	391.00	392.62	391.36	394.84	274.97
t_s (min)	30.04	29.92	29.90	29.84	29.78	17.58
t_f (min)	54.61	55.41	55.24	56.21	58.28	64.60
t_m (min)	35.50	36.11	36.28	36.16	36.51	24.46
$\Delta t_{1/2}$ (min)	7.84	7.50	8.42	7.80	7.90	25.42
DTG_{max} (wt %/min)	7.14	7.07	6.33	6.41	6.24	2.17
DTG_{mean} (wt %/min)	2.49	2.35	2.29	2.14	1.973	1.08

Table 5. Combustion Performance Parameters of Sludge, Lignite, and Mixed Samples

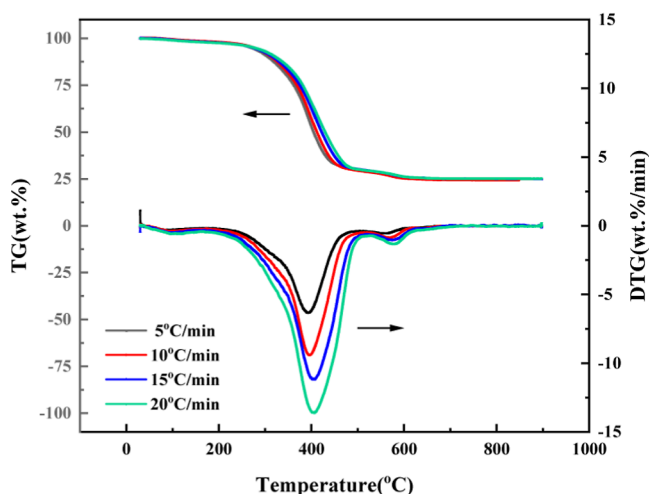| combustion characteristics	MDM	5 wt %	10 wt %	15 wt %	20 wt %	CYW
T_s (°C)	329.95	328.80	328.62	327.96	327.44	206.77
T_f (°C)	574.35	582.20	580.62	590.16	610.84	674.37
C_s*10^2 (wt %/min³)	0.67	0.66	0.58	0.59	0.57	0.50
C_f*10^3 (wt %/min⁴)	0.47	0.47	0.38	0.40	0.37	0.05
$S*10^7$ (wt %²/(°C³ min²))	2.84	2.63	2.31	2.16	1.88	0.81

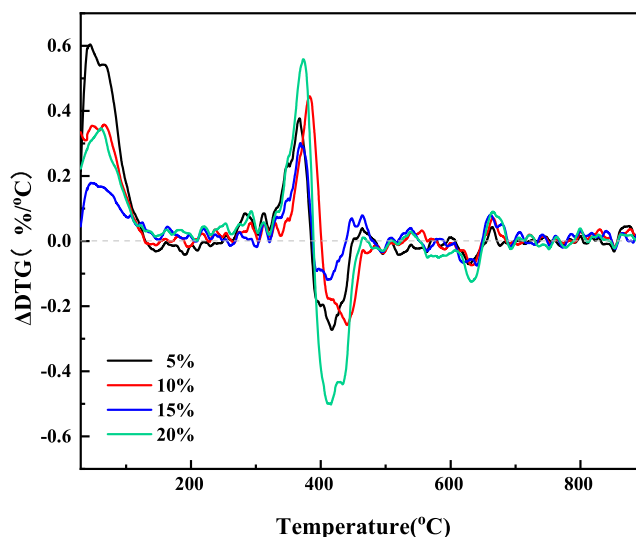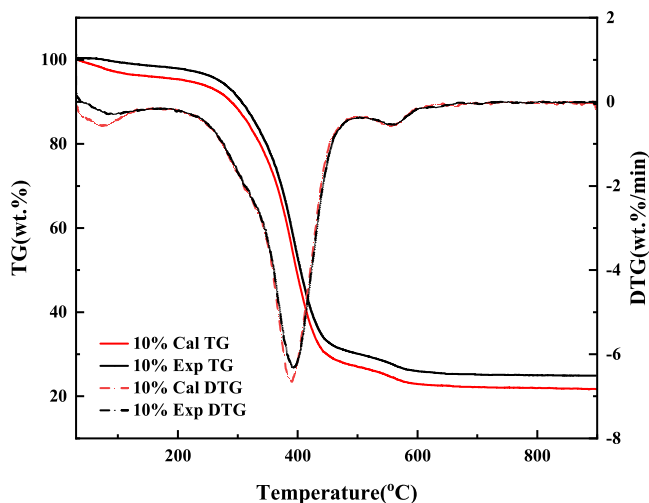**Figure 3.** TG and DTG curves for combustion of 10% blended fuels at different heating rates.

Figure 5. Variation curves of ΔDTG for four mixed samples.

Figure 4. Actual vs calculated TG-DTG curves for 10% blended fuels.

sludge contributes to ignition. When the sludge mass ratio was 5∼10 wt %, the combustion temperature did not change much compared to lignite. In addition, the combined combustion index showed a significant decrease with increasing sludge mixing ratio, from 2.63×10^{-7} wt %²/(°C³min²) for 5 wt % to 1.88×10^{-7} wt %²/(°C³min²) for 20 wt %. In particular, the combined combustion index decreased the most during sludge blending from 10 to 15 wt %, which also indicates that the combustion performance of blended fuels deteriorates by adding too much sludge up to a certain amount. In summary, the combustion performance of the 5−10 wt % blends differed less from that of lignite. The ignition and burnout temperatures of the 10 wt % blend are close to those of the lignite

samples, favoring fuel ignition and burnout. Therefore, it is reasonable to blend 10 wt % coal slurry samples into the coal.[21]

3.3. Analysis of the Effect of Heating Rate on the Combustion of Sludge and Lignite Mixture. Figure 3 displays the TG curves of mixed 10 wt % samples heated at four different rates. The typical temperature point shifts toward the high-temperature area as the heating rate rises, allowing the stabilized active structures to engage in the oxidation reaction earlier. In the next step of the oxidative combustion reaction, the reactive groups that did not have enough opportunity to react in the previous stage participate as the rate of temperature increase rises, leading to nonhomogeneous ignition and delaying the sample's combustion. It can be seen that the heating rate does not affect the thoroughness of mixed combustion, but it has an effect on the combustion process; that is to say, the larger the heating rate is, the more violent the combustion process is, and the larger the initial, peak, and burnout temperatures are. The maximum weight loss and peak temperature of the 10 wt % sample increased by 3.9 wt %/min and 20.14 °C, respectively, when the rate of temperature increase was increased from 10 to 25 °C/min.

3.4. Analysis of the Synergistic Effect of Mixed Combustion of Sludge and Lignite. From Figure 4, it can be observed that the suppression of the shoulder peaks increases as the sludge blending ratio increases. The mechanism by which coal and sludge inhibit the weight loss of organic substances with strong chemical bonds, such as semiaromatic compounds, is not clear and may be related to the minerals in coal and sludge.[22] By comparing the DTG curves of the measured/calculated values, the measured value of weight loss was 3.27% lower than the calculated value when the sludge blending ratio was 10 wt %. This is due to the sludge semicoke adhering to the coal surface and inhibiting the
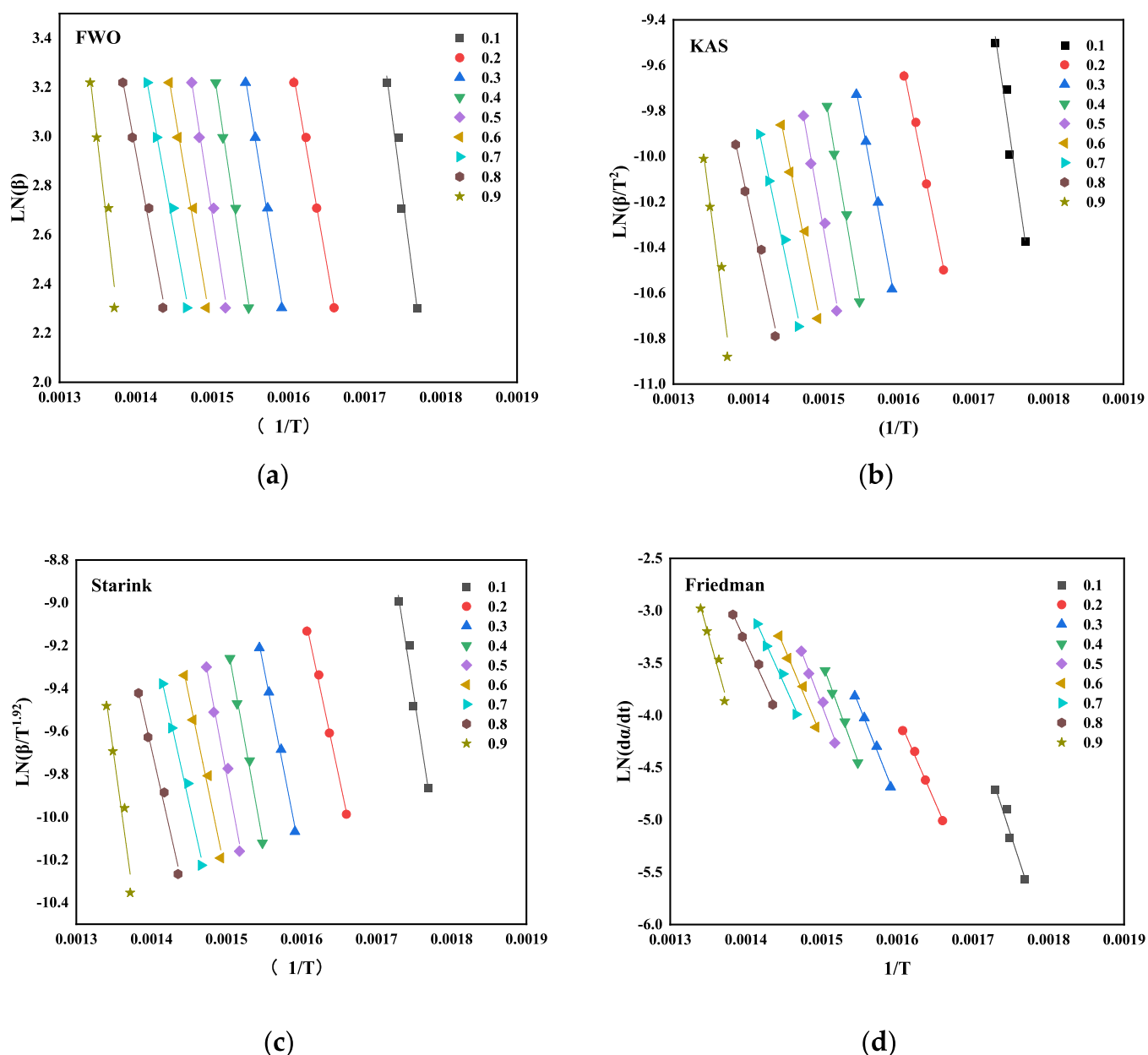
Figure 6. Linear fits under four kinetic models for different warming rates of 10% fuel blends. (a) FWO, (b) KAS, (c) Starink, and (d) Friedman.

Table 6. Activation Energy E and Correlation Coefficient R^2 for the Four Methods of Sludge, Lignite, and Mixed Fuels

sample	FWO		KAS		Starink		Friedman	
	E	R^2	E	R^2	E	R^2	E	R^2
5 wt %	157.77	0.973	155.02	0.970	155.33	0.970	157.86	0.970
10 wt %	134.74	0.990	130.77	0.988	131.11	0.988	133.37	0.989
15 wt %	157.99	0.933	155.25	0.923	155.56	0.924	157.88	0.922
20 wt %	184.27	0.917	182.94	0.909	183.23	0.909	185.70	0.911
MDM stage I	180.93	0.965	179.40	0.961	179.69	0.961	182.87	0.961
CYW stage I	169.40	0.825	168.95	0.805	169.19	0.806	157.93	0.783
CYW stage II	142.26	0.908	137.80	0.891	138.16	0.892	140.44	0.894

release of volatile matter. The two TG curves are significantly different, and there is a clear interaction.

As can be seen in Figure 5, there are multiple positive and negative peaks of ΔDTG, indicating inhibition and synergistic effects at different temperature intervals. Excluding the effect of moisture around 100 °C, smaller mixing and burning

interactions occurred in all the blends when the temperature was below 300 °C. Subsequently, ΔDTG starts to increase slightly with temperature and peaks at around 370 °C, indicating some inhibition during the mixing and burning process. Copolymers exhibit inhibitory rather than synergistic effects in this temperature range. This may be due to the fact
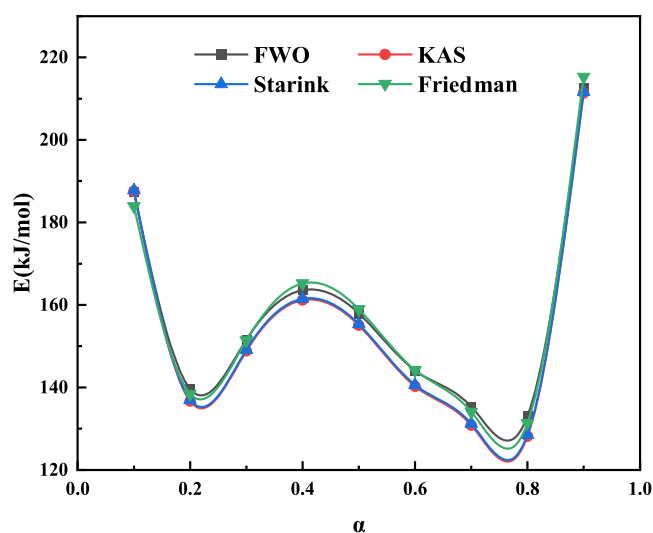
Figure 7. Trend of activation energy E for the four kinetic models.

that, currently, unbreakable components of the sludge impede the coal deashification process. Subsequently, the ΔDTG of the blends decreased rapidly and showed a negative value of ΔDTG in the temperature interval from 390 to 460 °C, showing a synergistic effect. It is worth noting that this temperature range is the most intense phase of lignite deashing and fixed carbon combustion. This overlapping temperature may be due to the fact that lignite releases a large amount of free radical volatiles at 390−460 °C, which improves the reactivity of light organic matter in the sludge.[23] The strong inhibition effect dominates the decomposition reaction of all the comonomers when the temperature ranges from 460 to 490 °C. Subsequently, the deviation of DTG decreases sharply, and the catalytic influence of metal-bearing minerals in the sludge on the mixing and burning process, which is noticeable in the coke oxidation stage, is responsible for the synergistic effect between 600 and 620 °C. Other researchers have discovered that metal-bearing minerals, particularly alkali and alkaline earth metals, have a catalytic influence on miscibility.[24] The weight loss of the peaks increased significantly when the sludge was mixed at 20 wt %, suggesting that there are strong interactions between the fuel blends at this ratio that promote the decomposition of more chemically bonded organic substances. The decomposition rate of more strongly bonded organic substances from mixed combustion is higher than the calculated value.

3.5. Kinetic Analysis. Based on the DTG curves, the kinetic parameters of sludge, lignite, and mixed samples were

calculated by selecting the most intense phase of the reaction. In the DTG curve, the temperature corresponding to a continuous steady decrease is the starting point, and the temperature corresponding to a continuous steady increase is the ending point. As shown in Figure 1, the combustion of lignite and the combustion of mixed samples have only one stage. Sludge combustion is divided into two stages. Higher values of E_α indicate higher intermolecular forces between the sample molecules and higher energy required for the reaction.[25] Four models, FWO, KAS, Starink, and Friedman, were used to estimate the reaction activation energy E_α for each sample. Plotting with origin as shown in Figure 6, the $\ln(\beta)$ versus $1/T$, $\ln(\beta^2)$ versus $1/T$, $\ln(\beta^{1.92})$ versus $1/T$, and $\ln(d\alpha/dt)$ versus $1/T$ curves, were plotted, and the activation energy of the reaction, E_α, was estimated by fitting the slopes.

From Table 6, calculate the activation energy E and correlation coefficient R^2 for the four methods for sludge, lignite, and mixed samples. Lignite combustion requires more activation energy than sludge, and the value of E decreases and then increases with an increasing sludge mixing ratio. The average activation energy of the four methods reached a minimum of 132.50 kJ/mol at a sludge blending ratio of 10 wt %, suggesting that the combustion of sludge blended with lignite is facilitated at this ratio. It is worth mentioning that the activation energy required for a sludge blending ratio of 20 wt % is rather greater than that of the pure lignite sample, which also suggests that excessive blending leads to fuel degradation. The correlation coefficients for each of these samples ranged between 0.91 and 0.99 (except for sludge), with strong linear relationships and reasonable results.

From Figure 7, it can be seen that the values of the reaction activation energy estimated by the different methods deviate by less than 5%. The average activation energy estimated based on the four models FWO, KAS, Starink, and Friedman has a gradual upward and then downward trend ($\alpha = 0.2 − 0.8$), with the same trend of change, and that sludge and lignite combustion is a complex reaction process. The activation energy tends to increase as the main chain is gradually decomposed with increasing conversion. Also, the activation energy decreases gradually due to the degradation of fixed carbon.

As can be seen from Table 7, the experimental data at the four temperatures are quite different, but the activation energies derived from the four methods are only slightly different and have the same trend. As the degree of conversion α increases from 0.1 to 0.9, the activation energy changes by a smaller amount. Meanwhile, all of the corresponding correlation coefficients are between 0.97 and 0.99 (0.2−0.8),

Table 7. Calculated Activation Energies and Correlation Coefficients for Four Methods for 10% Blended Fuels

| α	FWO		KAS		Starink		Friedman	
	E_α kJ/mol	R^2	E_α kJ/mol	R^2	E_α kJ/mol	R^2	E_α kJ/mol	R^2
0.1	187.30	0.927	187.53	0.934	187.76	0.928	183.89	0.922
0.2	139.57	0.993	136.65	0.994	136.95	0.993	138.40	0.992
0.3	151.56	0.994	148.84	0.995	149.14	0.994	151.42	0.994
0.4	163.58	0.992	161.19	0.993	161.50	0.992	165.22	0.992
0.5	157.95	0.979	155.04	0.982	155.36	0.979	158.93	0.981
0.6	144.09	0.978	140.26	0.982	140.60	0.979	144.14	0.980
0.7	135.35	0.978	130.84	0.982	131.20	0.978	134.10	0.980
0.8	133.05	0.979	128.17	0.983	128.54	0.979	131.35	0.981
0.9	212.56	0.922	211.35	0.930	211.68	0.923	215.29	0.926
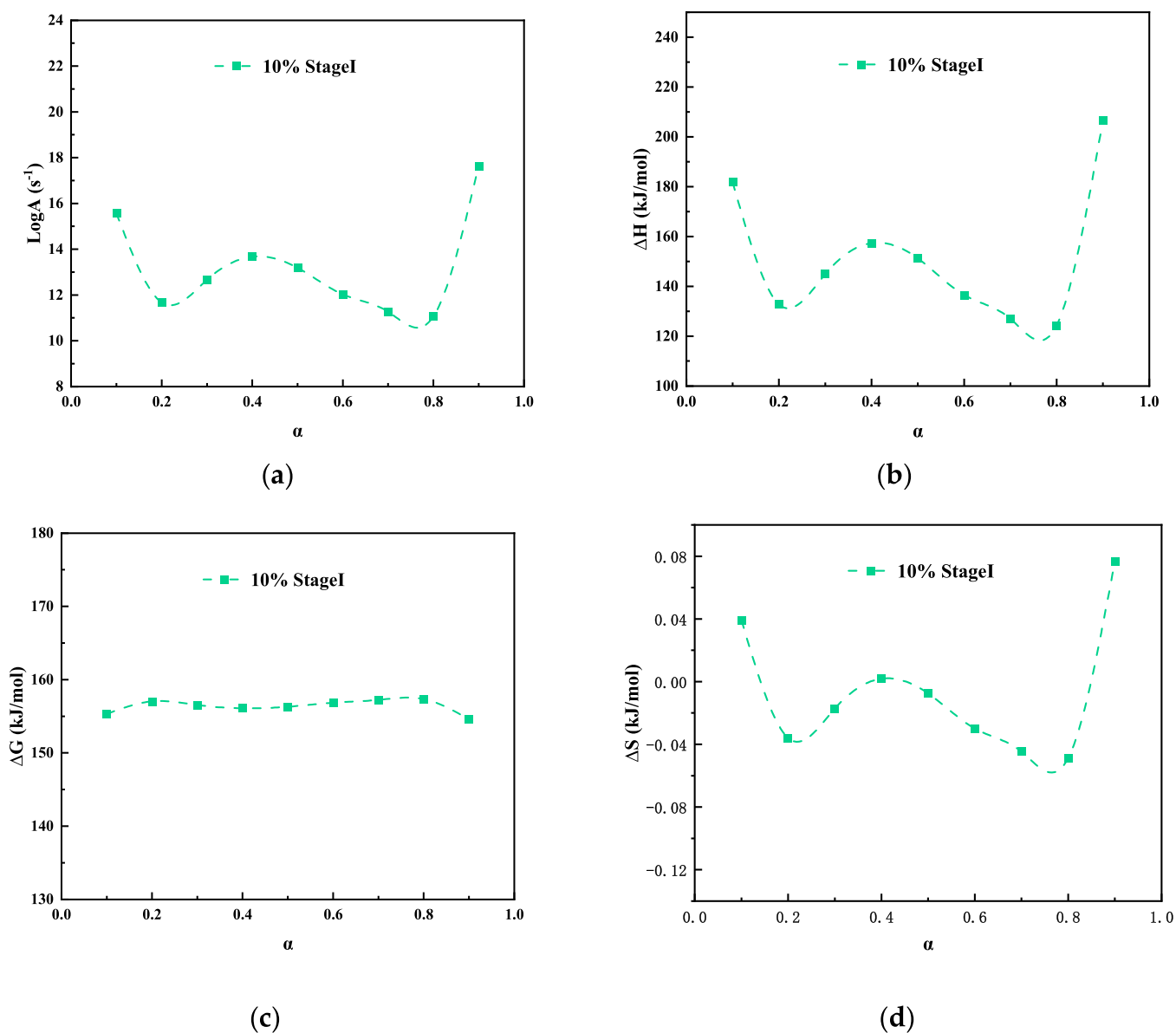
Figure 8. Variation curves of thermodynamic parameters (ΔG, ΔS, ΔH, and A) for 10% blended fuel (a) A, (b) ΔH, (c) ΔG, and (d) ΔS.

which is a strong linear relationship, indicating that the estimation results are reasonable. Among them, the KAS correlation coefficient, R^2 was the best fit.

3.6. Thermodynamic Analysis of Combustion. The thermodynamic parameters (ΔG, ΔS, ΔH, and A) were estimated using four methods at 20 °C/min, as shown in Figure 8. The ΔH value is a measure of the energy difference between the reactant and the activated complex. Also, the smaller the difference, the more thermodynamically favorable the generation of activated complexes and products. The enthalpies of 10% blended fuels were obtained by four methods, FWO, KAS, Starink, and Friedman, as 127.09~152.34, 122.21−155.70, 122.58~156.01, and 125.39~159.73 kJ/mol (α = 0.2−0.8) and ΔH has a similar graphical trend to E_α, indicating the feasibility of the reaction. A value of E_α greater than the value of ΔH indicates that the product generated is more favorable.[26] The Gibbs free energy (ΔG, kJ/mol) expresses the energy that can be obtained from the pyrolysis of the sample under study. The lower the ΔG is, the more viable the reaction is, indicating that the reaction

requires less energy to maintain. From Figure 8, it can be seen that the ΔG changes of the four methods, FWO, KAS, Starink, and Friedman, are basically the same, and the output of energy during the reaction is almost constant.

The chemical reaction's inherent characteristics, regardless of the reaction's temperature and independent of the quantity of substances in the system, determine A as a measure of the frequency of reactant collisions. $A \geq 10^{-9}$ s^{-1} indicates a simple complexation reaction; otherwise, a complex closed or interfacial reaction.[27] From the figure, it can be seen that the finger forward factors for the 10 wt % mixed combustion samples are all greater than 10^{-9} s^{-1}, which indicates that the reaction is a simple complex process. Entropy change (ΔS, J/mol) directly reflects the degree of disorder in a system in response to a certain set of changing conditions. The calculated entropy values of the results obtained by the four methods, FWO, KAS, Starink, and Friedman, range from −0.04 to 0.04. Negative values of apparent entropy indicate that the combustion process is approaching thermodynamic equilibrium and forming stable products.
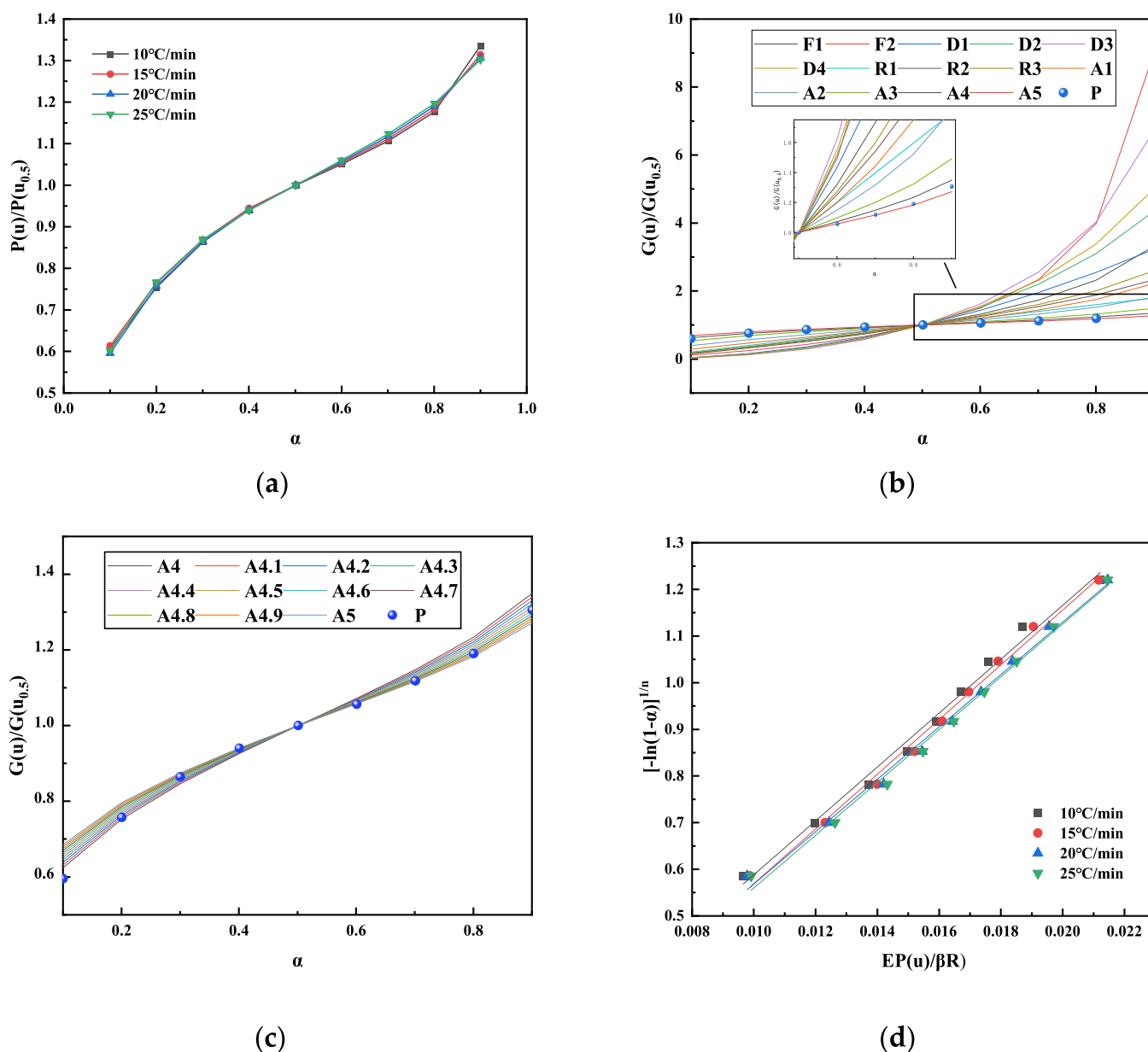
Figure 9. Reaction mechanism model for sludge and coal combustion $A_{4.2}$ at 10% fuel mixture. (a) $P(u)/P(u_{0.5})$. (b) Determine the reaction mechanism. (c) Determine the value of n. (d) Verification chart.

Table 8. Fitted Equations for Different Heating Rates for the 10% Blend $A_{4.2}$ Reaction Mechanism

temperature rise	$f(a)$	simultaneous equations	R^2
10 (°C/min)	$4.2_{/4.2}(1-\alpha)[-\ln(1-\alpha)]^{1-1}$	$Y = 57.77480x + 0.01039$	0.990
15 (°C/min)		$Y = 58.66776x - 0.01769$	0.992
20 (°C/min)		$Y = 56.16262x + 0.00651$	0.992
25 (°C/min)		$Y = 56.59595x - 0.00617$	0.993

The primary chemical mechanisms for the conversion between 0.1 and 0.9 can be seen in the figure. The average value of the activation energy determined via master plot analysis using the activation energy values calculated by the four methods was 156.95 kJ/mol. In order to find the most suitable reaction mechanism for the mixed combustion samples, the obtained reaction activation energy data and the corresponding temperature data were substituted into eq 16. A plot of $P(u)/P(u_{0.5})$ versus α-conversion degree ($\alpha = 0.1–0.9$) can be obtained for different heating rates. The $P(u)/P(u_{0.5})$ curves are very similar for the three heating rates, implying that the main reflection of mixed combustion can be described as a single irreversible reaction.[28]

Since the curves are essentially the same for different heating rates, the curve of $P(u)/P(u_{0.5})$ for the case of 20 °C/min was selected for comparison with the known theoretical model. Comparison of the theoretical $G(\alpha)/G(\alpha_{0.5})$ plots with the experimental $P(u)/P(u_{0.5})$ plots reveals that the main reflective mechanism function of sludge and lignite mixing and combustion belongs to model An, with the number of reaction stages between 4 and 5.

The expression for the number of reaction steps is

$$f(x) = n(1 - \alpha)[- \ln(1 - \alpha)]^{1-1/n} \qquad (20)$$

Combining this with the following relationship can be obtained

$$G(\alpha) = \frac{AE}{\beta R} p(u) = [- \ln(1 - \alpha)]^{1/n} \qquad (21)$$

The common reaction mechanisms and integral forms are combined in Table 3. The optimal reaction mechanism model is derived, as shown in Figure 9. To determine the value of n, it was decomposed at intervals of 0.1 to obtain a curve of $[-\ln(1 - \alpha)]^{1/n}$ versus $Ep(u)/\beta R$. The most appropriate response level, n, is the point in the graph where the ending is closest to zero and has the highest correlation coefficient. The correlation coefficient R^2 was found to be up to 0.992 when $n = 4.2$. A comparison of experimental and predicted values at different rates of warming was made, and the results were in agreement. As shown in Table 8, this leads to $A_{4.2}$ as the best reaction mechanism model for sludge and lignite at a 10 wt % blending ratio.

4. CONCLUSIONS

Based on the combined combustion indices of sludge, lignite, and blended fuels, it was concluded that the combustion performance of sludge increased significantly with the increase of the sludge blending ratio. Mixing a low-mass fraction of sludge with lignite can effectively improve the combustion performance of lignite and increase the lignite burnout temperature, but too much sludge will deteriorate the combustion process of lignite. The ignition and burnout temperatures of the 10 wt % blend were close to those of the lignite samples, and the combustion process had a strong synergistic effect in favor of fuel ignition and burnout. Therefore, it is reasonable to blend 10 wt % sludge samples in lignite. Additionally, the differences between the calculated and actual values of mass loss, residual fraction, and activation energy were calculated to illustrate the synergistic effect between the burning of sludge and the lignite mixture. The synergies between the sludges, as assessed by the mass loss curves, are reflected in the ash removal and coke oxidation stages.

TG combustion experiments were carried out using four different heating rates of 10, 15, 20, and 25 °C/min. The kinetic models of FWO, Starink, KAS, and Friedman were applied on the TG data to determine the E-values, where the KAS method had higher correlation coefficients, and the results were more plausible. The average activation energy E of mixed combustion at a 10 wt % mixing ratio of sludge and lignite was minimized to 132.50 kJ/mol, and A4.2 was the optimum reaction mechanism model. Subsequently, the thermal behavior of combustion was explored by analyzing the thermodynamic parameters (ΔG, ΔS, ΔH, and A). The reaction is judged to be a simple complexation reaction, with the combustion process approaching thermodynamic equilibrium and forming stable products.

ASSOCIATED CONTENT

Data Availability Statement

No data was used for the research described in the article.

AUTHOR INFORMATION

Corresponding Author

Yang Sun − *School of Energy and Environment, Shenyang Aerospace University, Shenyang 110000, China*; Phone: +862489723947; Email: sunyang@sau.edu.cn

Authors

Hui Sun − *School of Energy and Environment, Shenyang Aerospace University, Shenyang 110000, China*; orcid.org/0009-0004-5069-217X

Tianhua Yang − *School of Energy and Environment, Shenyang Aerospace University, Shenyang 110000, China*

Yiming Zhu − *School of Energy and Environment, Shenyang Aerospace University, Shenyang 110000, China*

Rundong Li − *School of Energy and Environment, Shenyang Aerospace University, Shenyang 110000, China*; orcid.org/0000-0002-8669-5397

Complete contact information is available at:
https://pubs.acs.org/10.1021/acsomega.3c08541

Author Contributions

Y.S.: methodology, investigation, data curation, and writing−review and editing. H.S.: experimental, data processing, writing original draft, conceptualization, and methodology. T. Y.: writing−review and editing, supervision, and resources. Y. Z.: conceptualization, validation, and supervision. R. L.: formal analysis and writing−review and editing.

Notes

The authors declare no competing financial interest.

REFERENCES

(1) Fu, J.; Wu, X.; Liu, J.; Evrendilek, F.; Chen, T.; Xie, W.; Xu, W.; He, Y. Co-circularity of spent coffee grounds and polyethylene via co-pyrolysis: Characteristics, kinetics, and products. *Fuel* **2023**, *337*, 127061.

(2) Zhao, Z.; Wang, R.; Wu, J.; Yin, Q.; Wang, C. Bottom ash characteristics and pollutant emission during the co-combustion of pulverized coal with high mass-percentage sewage sludge. *Energy* **2019**, *171*, 809−818.

(3) Dong, H.; Jiang, X.; Lv, G.; Chi, Y.; Yan, J. Co-combustion of tannery sludge in a commercial circulating fluidized bed boiler. *Waste Manage.* **2015**, *46*, 227−233.

(4) Qi, X.; Song, G.; Song, W.; Yang, S.; Lu, Q. Combustion performance and slagging characteristics during co-combustion of Zhundong coal and sludge. *J. Energy Inst.* **2018**, *91* (3), 397−410.

(5) Wang, Z.; Hong, C.; Xing, Y.; Li, Y.; Feng, L.; Jia, M. Combustion behaviors and kinetics of sewage sludge blended with pulverized coal: With and without catalysts. *Waste Manage.* **2018**, *74*, 288−296.

(6) Wang, R.; Zhao, Z.; Qiu, L.; Liu, J. Experimental investigation of synergistic behaviors of lignite and wasted activated sludge during their co-combustion. *Fuel Process. Technol.* **2017**, *156*, 271−279.

(7) Park, J. M.; Keel, S.; Yun, J.; Yun, J. H.; Lee, S.-S. Thermogravimetric study for the co-combustion of coal and dried sewage sludge. *Korean J. Chem. Eng.* **2017**, *34* (8), 2204−2210.

(8) (8a) Ding, Z.; Chen, H.; Liu, J.; Cai, H.; Evrendilek, F.; Buyukada, M. Pyrolysis dynamics of two medical plastic wastes: Drivers, behaviors, evolved gases, reaction mechanisms, and pathways. *J. Hazard. Mater.* **2021**, *402*, 123472. (8b) Kirti, N.; Tekade, S. P.; Tagade, A.; Sawarkar, A. N. Pyrolysis of pigeon pea (Cajanus cajan) stalk: Kinetics and thermodynamic analysis of degradation stages via isoconversional and master plot methods. *Bioresour. Technol.* **2022**, *347*, 126440.

(9) Zhuikov, A. V.; Glushkov, D. O. Characteristics of the Joint Combustion of Brown Coal and Sewage Sludge under Nonisothermal Heating Conditions. *Solid Fuel Chem.* **2022**, *56* (5), 353−359.

(10) Kai, X.; Yang, T.; Shen, S.; Li, R. TG-FTIR-MS study of synergistic effects during co-pyrolysis of corn stalk and high-density polyethylene (HDPE). *Energy Convers. Manage.* **2019**, *181*, 202−213.

(11) Lin, Y.; Chen, Z.; Dai, M.; Fang, S.; Liao, Y.; Yu, Z.; Ma, X. Co-pyrolysis kinetics of sewage sludge and bagasse using multiple normal distributed activation energy model (M-DAEM). *Bioresour. Technol.* **2018**, *259*, 173−180.

(12) Cai, H.; Liu, J.; Xie, W.; Kuo, J.; Buyukada, M.; Evrendilek, F. Pyrolytic kinetics, reaction mechanisms and products of waste tea via TG-FTIR and Py-GC/MS. *Energy Convers. Manage.* **2019**, *184*, 436−447.

(13) Chen, T.; Li, X.; Yan, J.; Jin, Y. Polychlorinated biphenyls emission from a medical waste incinerator in China. *J. Hazard. Mater.* **2009**, *172* (2−3), 1339−1343.

(14) Hu, J.; Yan, Y.; Evrendilek, F.; Buyukada, M.; Liu, J. Combustion behaviors of three bamboo residues: Gas emission, kinetic, reaction mechanism and optimization patterns. *J. Clean. Prod.* **2019**, *235*, 549−561.

(15) Xia, H.; Wei, K. Equivalent characteristic spectrum analysis in TG-MS system. *Thermochim. Acta* **2015**, *602*, 15−21.

(16) Liu, X.; Chang, F.; Wang, C.; Jin, Z.; Wu, J.; Zuo, J.; Wang, K. Pyrolysis and subsequent direct combustion of pyrolytic gases for sewage sludge treatment in China. *Appl. Therm. Eng.* **2018**, *128*, 464−470.

(17) Chen, J.; Mu, L.; Jiang, B.; Yin, H.; Song, X.; Li, A. TG/DSC-FTIR and Py-GC investigation on pyrolysis characteristics of petrochemical wastewater sludge. *Bioresour. Technol.* **2015**, *192*, 1−10.

(18) Liu, J.; Jiang, X.; Shen, J.; Zhang, H. Pyrolysis of superfine pulverized coal. Part 1. Mechanisms of methane formation. *Energy Convers. Manage.* **2014**, *87*, 1027−1038.

(19) Folgueras, M. B.; Díaz, R. Influence of FeCl3 and lime added to sludge on sludge-coal pyrolysis. *Energy* **2010**, *35* (12), 5250−5259.

(20) Folgueras, M. B.; Díaz, R. M.; Xiberta, J.; Prieto, I. Thermogravimetric analysis of the co-combustion of coal and sewage sludge. *Fuel* **2003**, *82* (15−17), 2051−2055.

(21) Tian, B.; Qiao, Y.; Bai, L.; Feng, W.; Jiang, Y.; Tian, Y. Pyrolysis behavior and kinetics of the trapped small molecular phase in a lignite. *Energy Convers. Manage.* **2017**, *140*, 109−120.

(22) Zhai, Y.; Zhu, Y.; Cui, S.; Tao, Y.; Kai, X.; Yang, T. Study on the co-pyrolysis of oil shale and corn stalk: Pyrolysis characteristics, kinetic and gaseous product analysis. *J. Anal. Appl. Pyrolysis* **2022**, *163*, 105456.

(23) Li, S.; Chen, X.; Liu, A.; Wang, L.; Yu, G. Co-pyrolysis characteristic of biomass and bituminous coal. *Bioresour. Technol.* **2015**, *179*, 414−420.

(24) (24a) Zou, C.; Wen, L.; Zhang, S.; Bai, C.; Yin, G. Evaluation of catalytic combustion of pulverized coal for use in pulverized coal injection (PCI) and its influence on properties of unburnt chars. *Fuel Process. Technol.* **2014**, *119*, 136−145. (24b) Gong, X.; Guo, Z.; Wang, Z. Variation on anthracite combustion efficiency with CeO2 and Fe2O3 addition by Differential Thermal Analysis (DTA). *Energy* **2010**, *35* (2), 506−511. (24c) Menares, T.; Herrera, J.; Romero, R.; Osorio, P.; Arteaga-Pérez, L. E. Waste tires pyrolysis kinetics and reaction mechanisms explained by TGA and Py-GC/MS under kinetically-controlled regime. *Waste Manage.* **2020**, *102*, 21−29.

(25) Zou, H.; Evrendilek, F.; Liu, J.; Buyukada, M. Combustion behaviors of pileus and stipe parts of Lentinus edodes using thermogravimetric-mass spectrometry and Fourier transform infrared spectroscopy analyses: Thermal conversion, kinetic, thermodynamic, gas emission and optimization analyses. *Bioresour. Technol.* **2019**, *288*, 121481.

(26) Aboulkas, A.; El harfi, K.; El Bouadili, A. Thermal degradation behaviors of polyethylene and polypropylene. Part I: Pyrolysis kinetics and mechanisms. *Energy Convers. Manage.* **2010**, *51* (7), 1363−1369.

(27) Maia, A. A. D.; de Morais, L. C. Kinetic parameters of red pepper waste as biomass to solid biofuel. *Bioresour. Technol.* **2016**, *204*, 157−163.

(28) Irmak Aslan, D.; Parthasarathy, P.; Goldfarb, J. L.; Ceylan, S. Pyrolysis reaction models of waste tires: Application of Master-Plots method for energy conversion via devolatilization. *Waste Manage.* **2017**, *68*, 405−411.